ACS APPLIED MATERIALS & INTERFACES

Research Article

www.acsami.org

New Low Molecular Weight Polycation-Based Nanoparticles for Effective Codelivery of pDNA and Drug

Yu Zhao,[†] Bingran Yu,*[,†] Hao Hu,[†] Yang Hu,[†] Na-Na Zhao,[†] and Fu-Jian Xu*[,†,‡,§]

[†]State Key Laboratory of Chemical Resource Engineering, College of Materials Science and Engineering, Beijing University of Chemical Technology, Beijing 100029, China

[‡]Beijing Laboratory of Biomedical Materials, Beijing University of Chemical Technology, Beijing 100029, China

[§]Key Laboratory of Carbon Fiber and Functional Polymers (Beijing University of Chemical Technology), Ministry of Education, Beijing 100029, China

Supporting Information

ABSTRACT: The development of new cationic nanoparticles that are safe and effective for biomedical applications has attracted considerable attention. Low molecular weight polycations generally exhibit low toxicity; however, their poor efficiency in drug delivery systems hampers their application. In this work, a series of new low molecular weight 2,6-bis(1-methylbenzimidazolyl)pyridinyl (BIP)-terminated ethanolamine-functionalized poly(glycidyl methacrylate)s (BIP-PGEAs) were readily fabricated for effective codelivery of a gene and a drug. The BIP-PGEAs could form well-defined cationic nanoparticles (NPs) in an aqueous solution. They could effectively bind pDNA with an appropriate particle size and ζ-potential. More importantly, the BIP-PGEA NPs demonstrated much higher transfection efficiencies than linear PGEA (L-PGEA) and the traditional "gold-standard" branched polyethylenimine (25 kDa). Moreover, the BIP-PGEA NPs could effectively entrap a hydrophobic anticancer drug such as 10-hydroxy camptothecin (CPT). The synergistic antitumor effect of the BIP-PGEA-CPT NPs was demonstrated by employing a suicide gene therapy system, which contained cytosine deaminase and 5-fluorocytosine (CD/5-FC). The present strategy for preparing well-defined cationic nanoparticles from low-molecular-weight polycations could provide an intriguing method to produce new multifunctional, therapeutic NPs.

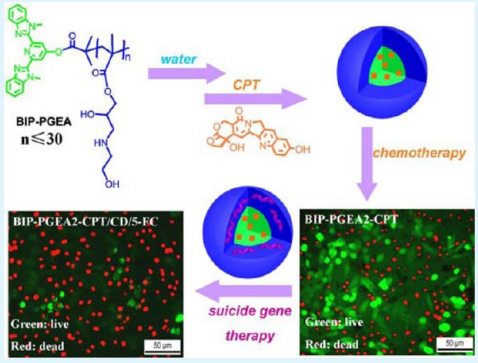

KEYWORDS: *gene vector, nanoparticles, amphiphilic polymers, ATRP, delivery*

INTRODUCTION

Gene therapy has been investigated for potential applications such as in curing cancer, the medical treatment of infection and innate immunodeficiency, as well as cardiovascular diseases.[1,2] Instead of virus-based vector systems, increasing efforts have been made to design different cationic polymers as nonviral gene carriers.[3−7] High-molecular-weight polycations, which can effectively condense pDNA to be a stable polyplex, were intensively investigated as nonviral vectors.[5,8] A large number of polycations such as polyethylenimine (PEI),[9−14] poly(2-(dimethylamino)ethyl methacrylate),[9,15] poly(L-lysine),[16] poly(aspartic acid),[17,18] and polyamidoamine[19] have been utilized as gene vectors. As reported in our earlier works,[20,21] a ethanolamine (EA)-functionalized poly(glycidyl methacrylate) (PGMA) vector (denoted as PGEA) could efficiently mediate gene delivery in some cell lines while exhibiting very low toxicity.[20−25]

However, the current knowledge and understanding in the gene delivery field are still preliminary and insufficient for clinical application.[26,27] The development of new cationic nanoparticles that are safe and effective for biomedical applications have recently attracted considerable attention.[11,28−30] Great efforts have been made to explore the combination of gene therapy and chemotherapy.[31−33] It has been reported that the codelivery of drugs and genes could be realized using self-assemblies from amphiphilic, cationic copolymers.[34,35] A further reduction in cytotoxicity and an increase in efficiency of the polycation-based assemblies would facilitate their application.

In general, low molecular weight polycations exhibit low toxicity; however, their poor delivery efficiency hampers their use in biomedical applications. In this work, we report that low molecular weight 2,6-bis(1-methylbenzimidazolyl) pyridinyl (BIP)-terminated PGEAs (BIP-PGEAs) could form new cationic nanoparticles (NPs) in aqueous solutions for effective codelivery of genes and drugs (Figure 1). The BIP (a π-conjugated, hydrophobic molecule) core of the BIP-PGEA NPs acts as a hydrophobic drug container, whereas the PGEA periphery can carry pDNA. The physicochemical properties of the BIP-PGEAs including pDNA condensation capability,

Received: July 15, 2014
Accepted: September 23, 2014
Published: September 23, 2014

   dx.doi.org/10.1021/am5046179 | ACS Appl. Mater. Interfaces 2014, 6, 17911−17919

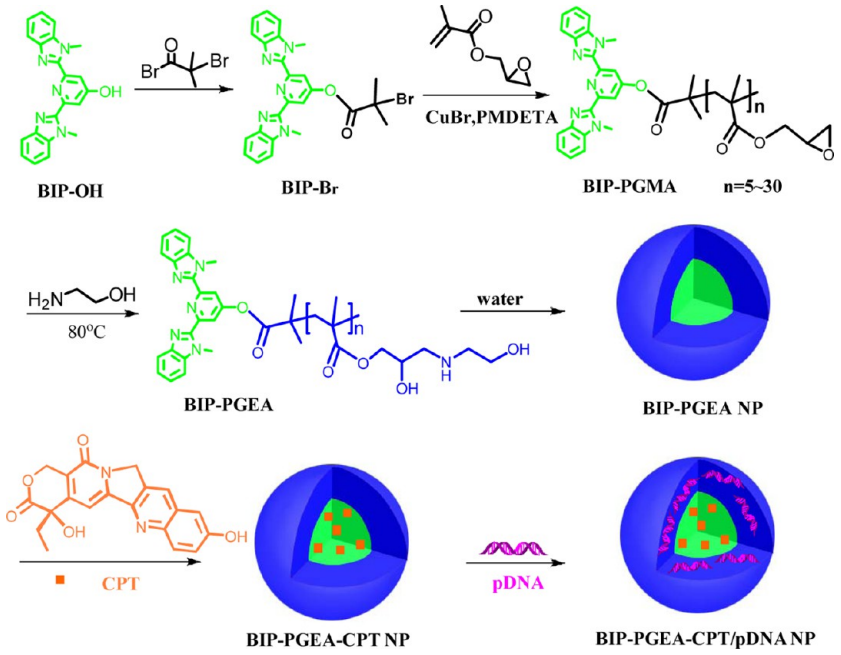

Figure 1. Preparation processes of the BIP-PGEA-CPT/pDNA complexes.

cytotoxicity, and gene transfection were examined in detail. A model hydrophobic drug (10-hydroxy camptothecin (CPT)) was encapsulated into the BIP-PGEA NPs. The release behavior of CPT was also investigated. A suicide gene/prodrug system has been demonstrated to be effective in treating radioresistant and chemoresistant tumors.[36,37] The synergistic antitumor effect of the BIP-PGEA-CPT NPs was demonstrated using a cytosine deaminase/5-fluorocytosine (CD/5-FC) suicide gene therapy system.

EXPERIMENTAL SECTION

Materials. Branched polyethylenimine (PEI, M_w ~ 25 000 Da), glycidyl methacrylate (GMA, 98%), ethanolamine (EA, 98%), 2,6-dicarboxy-4-hydroxypyridine, N,N,N′,N″,N″-pentamethyldiethylenetriamine (PMDETA, 99%), 2-bromoisobutyryl bromide (BIBB, 98%), ethyl bromoisobutyrate (99%), fluorescein diacetate (FDA, 98%), 3-(4,5-dimethylthiazol-2yl)-2,5-diphenyl tetrazolium bromide (MTT), propidium iodinate (PI, 98%), and copper(I) bromide (CuBr, 99%) were purchased from Sigma-Aldrich Chemical Co., St. Louis, MO. 2,6-Bis(1-methylbenzimidazolyl)-4-hydroxypyridine (BIP−OH) was prepared by procedures reported earlier.[38] GMA was used after removal of the inhibitors. The plasmid pRL-CMV encoding *Renilla* luciferase (Promega Co., Cergy Pontoise, France), the plasmid pEGFP-N1 encoding enhanced green fluorescent protein (EGFP) (BD Biosciences, San Jose, CA), and the plasmid pAdTrack-CMV-CD (pCMVCD) encoding *Escherichia coli* cytosine deaminase (ECD) were amplified in *Escherichia coli* and purified according to the supplier's protocol (Qiagen GmbH, Hilden, Germany).

Synthesis of [2,6-Bis(1-methylbenzimidazolyl)-4-yl]-2-bromo-2-methylpropanoate (BIP-Br). BIP-OH (355 mg, 1 mmol) was added into a 50 mL round flask containing 8 mL of DMF and a magnetic stirrer. After the BIP-OH was thoroughly dissolved, BIBB (0.5 mL, 4 mmol) was added dropwise into the aforementioned solution under ice bath conditions. The reaction was conducted at room temperature for 24 h. The BIP-Br was precipitated in an excess of diethyl ether, dried under reduced pressure for 12 h to remove residual diethyl ether and isolated as a white solid (454 mg, 90% yield). ^{1}H NMR (400 MHz, $CDCl_3$, Me_4Si) δ = 4.32 (s, 6H), 7.38 (m, 4H), 7.46 (d, $^3J_{(H,H)}$ = 8.0 Hz, 2H), 7.86 (d, $^3J_{(H,H)}$ = 8.0 Hz, 2H), 8.30 (s, 2H); ^{13}C NMR (100 MHz, $CDCl_3$, Me_4Si) δ = 30.7, 32.7, 54.5, 110.2, 118.3, 120.5, 123.2, 124.1, 137.4, 142.7, 149.5, 151.9, 151.9, 159.1, 168.9. Electrospray ionization mass spectrometry (ESI-MS) was calculated for $[C_{46}H_{39}BrN_{10}O_3+H]^+$ 504.1035, 506.1015 and found 504.1038, 560.1020.

Synthesis of BIP-PGMA and Linear PGMA via ATRP. The BIP-PGMA polymers were synthesized under the typical conditions of ATRP.[39] BIP-Br (0.15 g, 0.30 mmol, 1 equiv), GMA (4.3 mL, 30 mmol, 100 equiv), and PMDETA (130 μL, 0.75 mmol, 2.5 equiv) were added into a 50 mL flask containing 5 mL of DMSO. The reaction system was degassed by nitrogen for 10 min before adding CuBr (42.8 mg, 0.30 mmol, 1 equiv) under a nitrogen atmosphere. The polymerization was conducted for 15 to 50 min at room temperature. The reaction was terminated by exposure to air. The BIP-PGMAs were precipitated in an excess of methanol to remove the catalyst complex. The crude polymer was dried under reduced pressure after being purified by reprecipitation cycles with methanol. The products of the ATRP reactions with polymerization times of 15, 30, and 50 min were named BIP-PGMA1 (M_n =1.14 × 10^3 g/mol, PDI = 1.21), BIP-PGMA2 (M_n = 2.32× 10^3 g/mol, PDI = 1.32), and BIP-PGMA3 (M_n = 4.47× 10^3 g/mol, PDI = 1.35), respectively.

For the preparation of the control linear PGMA (L-PGMA), GMA (3.5 mL, 100 equiv), ethyl bromoisobutyrate (160 μL, 1 equiv), and PMDETA (450 μL, 3 equiv) were added into a 50 mL flask containing 5 mL of DMSO. The reaction system was degassed by argon for 10 min before adding CuBr (115 mg, 0.8 mmol, 1 equiv). The following procedures were similar to those described above. The polymerization was conducted for 30 min. The molar weight of the final L-PGMA was 3.97× 10^3 g/mol (PDI = 1.24).

Synthesis of BIP-PGEA and L-PGEA. The procedures followed our previous work.[21] Briefly, 0.2 g of BIP-PGMA or L-PGMA was dissolved in 5 mL of DMSO, and then 3 mL of EA was added. The reaction mixture was stirred at 80 °C for 40 min. The crude product was purified using a dialysis membrane (MWCO 1000) prior to lyophilization.

Material Characterization. ^{1}H NMR and ^{13}C NMR spectra were recorded on a Bruker ARX 400 MHz spectrometer using $CDCl_3$ (for BIP-Br and BIP-PGMA) and D_2O (for BIP-PGEA) as the solvents and with tetramethylsilane (Me_4Si) as an internal standard. GPC measurements of BIP-PGMA and linear PGMA were performed on a Waters GPC system.[21] Dynamic light scattering (DLS) measurements were performed using a Zetasizer Nano ZS (Malvern Instruments, Southborough, MA) equipped with a laser of wavelength 633 nm and positioned at a 173° scattering angle. Transmission

electron microscopy (TEM) studies were conducted using a JEOL JEM 2010F at an acceleration voltage of 100 kV. The samples were prepared by drop-casting nanoparticle solutions onto carbon-coated copper grids and drying in air. Gel electrophoresis was implemented in a Sub-Cell system (Bio-Rad Laboratories). A UV transilluminator and BioDco-It imaging system (UVP Inc.) was employed to record the DNA bands. UV−vis measurements were monitored on a SHIMADZU UV-2600 UV−vis spectrometer from 200 to 800 nm.

Preparation of BIP-PGEA/pDNA. As in our earlier work,[39] all of the polymer solutions were prepared in water at an nitrogen concentration of 10 mM. N/P ratios were defined to express the polymer to pDNA ratios as molar ratios of the nitrogen (N) in BIP-PGEA to the phosphate (P) in pDNA. The average mass weight per phosphate group of pDNA was approximately 325.[40] All of the BIP-PGEA/pDNA nanocomplexes with different N/P ratios were formed by mixing the BIP-PGEA solution and the pDNA solution for 30 min before use.

Cell Viability Assay. The cytotoxicity of the polymer vectors at series of N/P ratios in COS7 and HepG2 cells cultured in medium (with 10% FBS) was assessed using a MTT assay, as described in our previous work.[39,40] The final absorbance was recorded at a wavelength of 570 nm. The cell viability results were expressed as the percentage relative to that of the control.

In Vitro Transfection Assay. The in vitro gene transfection of the BIP-PGEA/pDNA complexes was first conducted in COS7 and HepG2 cells utilizing the plasmid pRL-CMV as the reporter gene.[21,39,40] Briefly, the COS7 and HepG2 cells were cultured in 24-well plates at a density of 6×10^4 cells/well with medium (with 10% FBS). The complexes (20 μL/well containing 1.0 μg of pDNA) at various N/P ratios were then added to the transfection medium. The enhanced green fluorescent protein (EGFP) pDNA was also used in HepG2 cells at the optimal N/P ratios of polycations using similar procedures.

Drug Loading and Release. CPT-loaded BIP-PGEA2 (BIP-PGEA2-CPT) NPs were prepared as follows. Under moderate stirring, BIP-PGEA2 (13.2 mg) from BIP-PGMA2 was dissolved in 7 mL of distilled water. CPT (1.4 mg) was dissolved into 1 mL of DMSO and then added dropwise to the above solution with moderate stirring. The π-conjugated plane of BIP interacts with the aromatic structure of CPT via noncovalent van der Waals interactions. After stirring for 12 h at 25 °C, the solution was dialyzed against deionized water (MWCO 1000) for 12 h. The resulting solution was centrifuged to remove uncoupled CPT and then lyophilized. Using this loading method, a considerable drug loading capacity could be obtained, as reported earlier.[41] UV−vis spectrophotometry at 380 nm was used to estimate the drug loading capability.[41−43]

Dialysis was used to investigate the release profile of CPT from BIP-PGEA2-CPT NPs. BIP-PGEA2-CPT NPs (2.5 mg) were dispersed into 5 mL of PBS (or deionized water) using a dialysis tube against 20 mL of PBS (or deionized water). The experiment proceeded at a constant temperature of 37 °C for 72 h. At each time interval, 3 mL of solution was removed from the tube and measured using UV−vis spectrophotometry at 380 nm. Then, an equal volume of fresh PBS (or deionized water) was supplemented accordingly. The cytotoxicity of free CPT and BIP-PGEA2-CPT in HepG2 cells was assessed using a MTT assay after 72 h of incubation.

Antitumor Effect Assay Using a 5-FC/ECD Suicide Gene Therapy System. The HepG2 cells were cultured in 96-well plates at an initial density of 1×10^4 cells/well. They were transfected as described above. At the time of transfection, the solution containing the BIP-PGEA2/pCMV-CD complexes (6.7 μL/well containing 0.33 μg of pDNA) at the optimal N/P ratio of 25 was added in 100 μL of growth medium. After 4 h of incubation under standard conditions, the transfection medium was replaced with 100 μL of fresh culture media, and 5-FC (0−160 μg/mL) was subsequently added. After 72 h of incubation, the cell viability was evaluated using the MTT assay. A rapid procedure using propidium iodide (PI) and fluorescein diacetate (FDA) was also employed to assess the cell viability of free CPT, 5-FC, BIP-PGEA2, and BIP-PGEA2-CPT in the HepG2 cells. FDA and PI were prepared using the method described earlier.[44]

RESULTS AND DISCUSSION

Synthesis and Characterization of BIP-PGEAs. BIP-PGEAs were synthesized according to the routes depicted in Figure 1. The starting bromoisobutyryl-terminated BIP (BIP-Br) initiator was synthesized via the direct reaction of the hydroxyl group of BIP-OH with 2-bromoisobutyryl bromide. The chemical structure of BIP-Br was characterized using ^{1}H NMR spectroscopy (Figure S1, see Supporting Information). The signal at δ = 2.10 ppm was associated with the methyl protons (e, C(Br)−CH_3) of the 2-bromoisobutyryl groups. The area ratio of peak e and peak a indicated that BIP−OH was completely converted into BIP-Br. As shown in Figure 1, well-defined BIP-PGMA conjugates were subsequently synthesized via ATRP of BIP-Br. The BIP-PGMAs with different lengths of PGMA were synthesized with different ATRP times. The molecular weights and distributions of the BIP-PGMAs were measured using GPC, as summarized in Table 1. In detail, the

Table 1. Characterization of the Polycations

sample	reaction time of ATRP (min)	M_n (g/mol)[c]	PDI[c]	monomer repeat units per chain	
BIP-PGMA1[a]	15	1.14×10^3	1.21	4[d]	5[e]
BIP-PGMA2[a]	30	2.32×10^3	1.32	13[d]	15[e]
BIP-PGMA3[a]	50	4.47×10^3	1.35	29[d]	30[e]
L-PGMA[b]	30	3.97×10^3	1.24	32[d]	

[a]Synthesized using a molar feed ratio [GMA (4.3 mL)]/[BIP-Br (150 mg, 0.30 mmol)]/[CuBr (42.8 mg, 0.30 mmol)]/[PMDETA (130 μL, 0.75 mmol)] of 100:1:1:2.5 in 5 mL of DMSO. [b]Synthesized using a molar feed ratio [GMA (3.5 mL)]/[ethyl bromoisobutyrate (160 μL)]/[CuBr (120 mg, 0.83 mmol)]/[PMDETA (450 μL, 2.5 mmol)] of 100:1:1:3 in 5 mL of DMSO. [c]Determined from GPC results. PDI = weight-average molecular weight/number-average molecular weight, or M_w/M_n. [d]Determined from M_n and the molecular weights of BIP-Br (504 g/mol) and GMA (142 g/mol) . [e]Determined from the ^{1}H NMR data.

number-average molecular weights of BIP-PGMA1 from 15 min of ATRP, BIP-PGMA2 from 30 min of ATRP, and BIP-PGMA3 from 50 min of ATRP were 1.14×10^3, 2.32×10^3, and 4.47×10^3 g/mol with PDI values of 1.21, 1.32, and 1.35, respectively.

The ^{1}H NMR spectra of the BIP-PGMAs showed significant changes in comparison with that of the BIP-Br (Figure S1, Supporting Information). By referencing previous ^{1}H NMR studies on PGMA,[45] the peaks at δ = 3.23 (g), 2.84 (h), and 2.64 ppm (h) were clearly assigned to the protons of the epoxide ring. The area ratio of peaks f, g, and h was approximately 2:1:2, indicating that the epoxy groups in the PGMA did not change throughout the polymerization processes. In addition, the signal at δ = 8.21 ppm was assigned to the two protons (a) of the pyridyl ring of BIP. The degree of polymerization (DP) could be determined according to the following equation: DP = 2A(g)/A(a), where A(a) and A(g) are the average integrals of peaks a and g, respectively. The DPs of the BIP-PGMAs were estimated to be 5, 15, and 30, respectively, which was fairly consistent with those determined using GPC (Table 1). Moreover, the molecular weight of the prepared control L-PGMA with approximately 32 repeat units was similar to that of BIP-PGMA3.

For the preparation of BIP-PGEA, the BIP-PGMAs were reacted with excess EA. After the ring-opening reactions, the peaks (f) at δ = 3.82 and δ =4.30 ppm (Figure S1c, Supporting Information) of the BIP-PGMA shifted to one peak at δ = 4.10 ppm (Figure S1d). The new peaks at δ =3.75 to 4.10 and δ = 2.83 ppm were mainly attributed to the methylidyne protons (CH−OH, g′) and methylene protons (CH_2−OH, f′ and NH−CH_2, h′), respectively. The area ratio of peaks h′ and g′ to f′ was approximately 4:5, indicating that all of the rings of the BIP-PGMAs were opened by EA. Furthermore, the resonances of BIP in the BIP-PGEAs were invisible (Figure S1d). This phenomenon indicated that the $\pi-\pi$ stacking interactions of BIP species made the BIP-PGEAs form nanoparticles in an aqueous solution (see below). Thus, only the resonance signals of the outward PGEA segments of the BIP-PGEA NPs were detected.

Physical Characterization of the BIP-PGEA/pDNA Complexes. Agarose gel electrophoresis, dynamic light scattering, and ζ-potential measurements were used to evaluate the ability of the BIP-PGEAs to condense pDNA. Dynamic light scattering was also employed to estimate the stability of the BIP-PGEA2/pDNA complex. TEM imaging was conducted to observe the morphologies of the resultant NPs. Figure 2

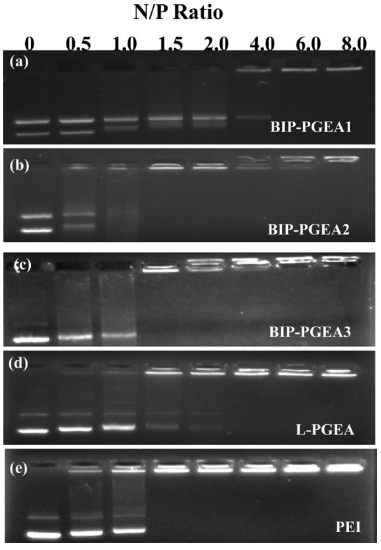

Figure 2. Electrophoretic mobilities of pDNA in the complexes with the cationic vectors ((a) BIP-PGEA1, (b) BIP-PGEA2, (c) BIP-PGEA3, (d) L-PGEA, and (e) PEI) at various N/P ratios.

shows the gel retardation results of the polymer/pDNA complexes with increasing N/P ratios in comparison with those of the control "gold-standard" PEI (25 kDa) and the L-PGEA (prepared from the control L-PGMA, Table 1). All of the BIP-PGEAs could compact pDNA at a N/P ratio of approximately 4. The condensation abilities of BIP-PGEA2 and BIP-PGEA3 were better than L-PGEA, which was comparable to that of PEI (compacted pDNA at a N/P ratio of 1.5).

The particle sizes of the pristine BIP-PGEA NPs ranged from 240 to 300 nm (Figure 3a). For the BIP-PGEA/pDNA complexes, their sizes depended on the N/P ratio. As the N/P ratio increased, the size of the complexes decreased. At a N/P ratio above 10, all of the BIP-PGEAs could condense pDNA into complexes with sizes less than 250 nm. Such complexes are suitable for endocytosis.[46] The ζ-potential values of the polymer/pDNA nanoparticles were all highly positive (20−40

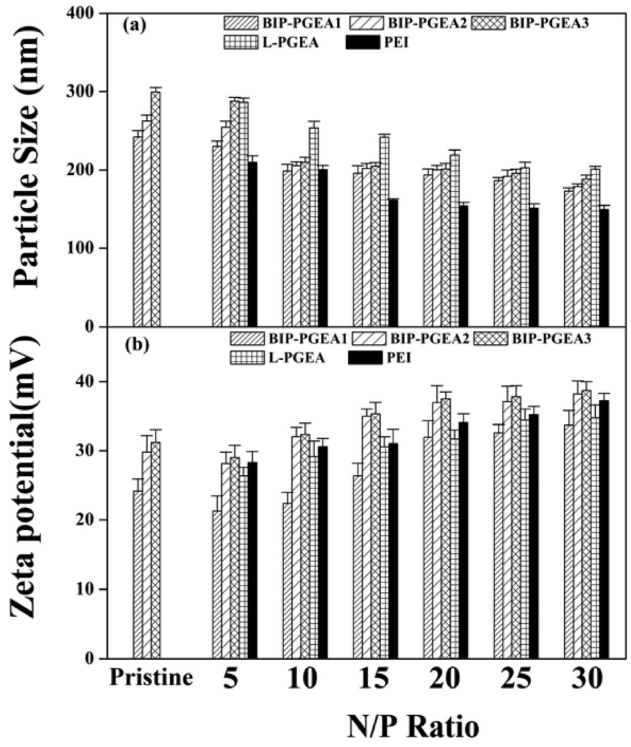

Figure 3. (a) Particle sizes and (b) ζ-potentials of the BIP-PGEA/pDNA, L-PGEA/pDNA, and PEI/pDNA complexes at various N/P ratios compared with those of the pristine BIP-PGEAs.

mV) (Figure 3b), which would result in good affinities for negatively charged cell surfaces. The stability of the complexes in the presence of serum was also investigated. As shown in Figure S2 (Supporting Information), the particle sizes of the BIP-PGEA2/pDNA complexes at a N/P ratio of 25 in medium with 10% FBS were approximately 200 nm during an incubation time of 0−5 h. This result indicated that the complexes could be stable during the transfection process because the cellular uptake of the complexes was within the incubation time of 4 h.

The morphologies of the NPs were observed using TEM. Figure 4(a and b) shows typical images of BIP-PGEA2 and BIP-PGEA2/pDNA at a N/P ratio of 25. The compacted complexes exhibited identical nanoparticles of spherical shape. No obvious differences for the BIP-PGEA2 NPs before and after complexing with pDNA were observed.

Cell Viability Assay. Cytotoxicity is another important factor for delivery systems. Factors that affect the cytotoxicity of gene vectors include the molecular weight, structure and charge density of polycations.[42] The cytotoxicity of the BIP-PGEAs was investigated in comparison with those of the control L-PGEA and PEI in COS7 and HepG2 cells (Figure 5). As the N/P ratio increased, the cytotoxicity of the gene vectors increased. At higher N/P ratios, besides the compact and positively charged nanoparticles, the transfection system also contained free cationic polymers or particles, which would increase the cytotoxicity. The cytotoxicity was highly dependent on the molecular weight.[45] BIP-PGEA3 with the highest molecular weight showed the highest toxicity among the BIP-PGEAs at all of the N/P ratios. Notably, all of the BIP-PGEAs exhibited much lower cytotoxicity than the control "gold-standard" PEI (25 kDa). For example, at the N/P ratio of 20,

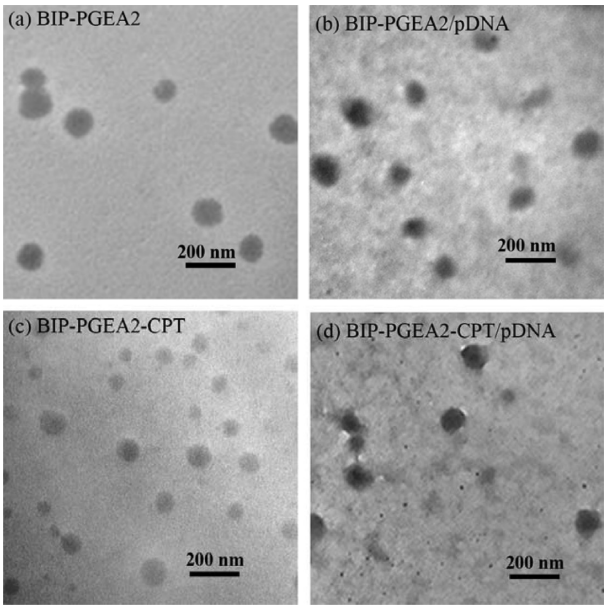

Figure 4. TEM images of (a) BIP-PGEA2, (b) BIP-PGEA2/pDNA at a N/P ratio of 25, (c) BIP-PGEA2-CPT, and (d) BIP-PGEA2-CPT/pDNA at a N/P ratio of 25.

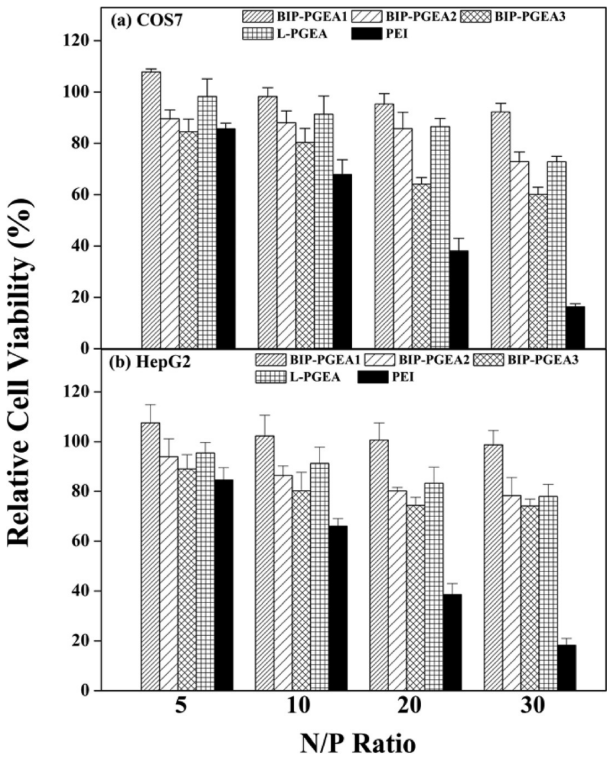

Figure 5. Cell viability of BIP-PGEA/pDNA and PEI/pDNA complexes at different N/P ratios in (a) COS7 and (b) HepG2 cells.

the cell viability of BIP-PGEA2 was above 80%, whereas it was only 30% for the cells treated with PEI.

Gene Transfection Assay. The gene transfection efficiency mediated by the BIP-PGEAs was analyzed at N/P ratios from 5 to 30 in COS7 and HepG2 cells. Figure 6 shows the profile of luciferase expression of BIP-PGEAs and L-PGEA at different N/P ratios in comparison with that of PEI (25 kDa) at its optimal N/P ratio of 10.[44,45,47] The N/P ratio greatly influenced the gene transfection efficiency. As the N/P ratio

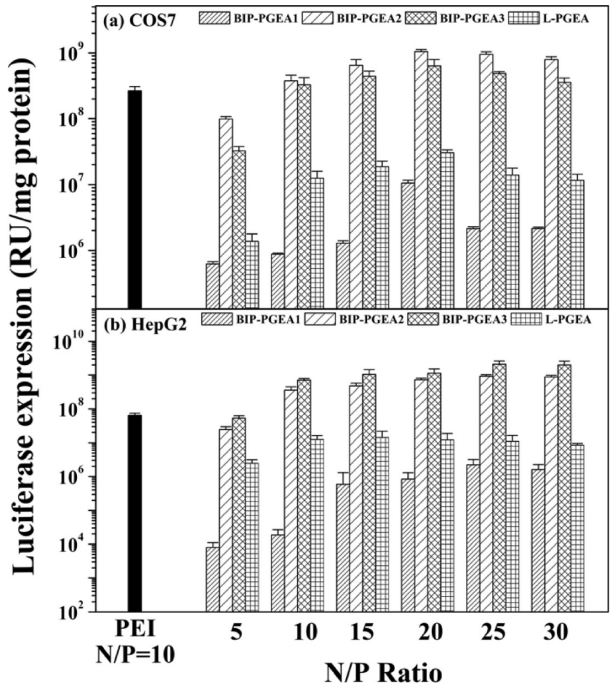

Figure 6. In vitro gene transfection efficiency of the BIP-PGEA/pDNA complexes at various N/P ratios compared with those of L-PGEA (at various N/P ratios) and PEI (25 kDa, at the optimal N/P ratio of 10) in (a) COS7 and (b) HepG2 cells.

increased, the transfection efficiency first increased and then slightly decreased. At lower N/P ratios, loose nanocomplexes formed because the pDNA could not be efficiently compacted by the cationic polymers that cannot easily enter the cell. The transfection efficiency decreased upon increasing the N/P ratio to greater than the optimal value, which may be caused by the increased toxicity of the nanoparticles at higher N/P ratios (Figure 5).

The transfection efficiency of the BIP-PGEAs was also dependent on the molecular weights. The BIP-PGEA2 and BIP-PGEA3 NPs with higher molecular weights possessed increased binding abilities and complex stabilities, likely leading to much higher transfection efficiencies. No obvious differences were observed in the efficiencies mediated by BIP-PGEA2 and BIP-PGEA3. The transfection efficiencies mediated by BIP-PGEA2 and BIP-PGEA3 in both cell lines at all of the N/P ratios were significantly higher than those of the control L-PGEA. As mentioned above, L-PGEA from L-PGMA possessed a similar molecular weight to that of BIP-PGEA3 from BIP-PGMA3 (Table 1). The greater gene delivery ability of BIP-PGEA2 and BIP-PGEA3 was likely due to their nanoparticle conformations from $\pi-\pi$ stacking. The BIP-PGEA2 and BIP-PGEA3 NPs could condense pDNA more effectively (Figure 2). Moreover, the transfection efficiencies of BIP-PGEA2 and BIP-PGEA3 at most of the N/P ratios were much higher than that of PEI at its optimal ratio of 10.

To visually compare the transfection abilities of the BIP-PGEA vectors, the plasmid pEGFP-N1 encoding GFP was also used in the HepG2 cells. Representative images of EGFP gene expression mediated by the BIP-PGEAs and L-PGEA under the optimal N/P ratio of 25 are shown in Figure 7. BIP-PGEA2 and BIP-PGEA3 presented a significantly higher number of green (EGFP-positive) HepG2 cells than BIP-PGEA1 and L-PGEA. The percentage of the EGFP-positive cells, qualitatively

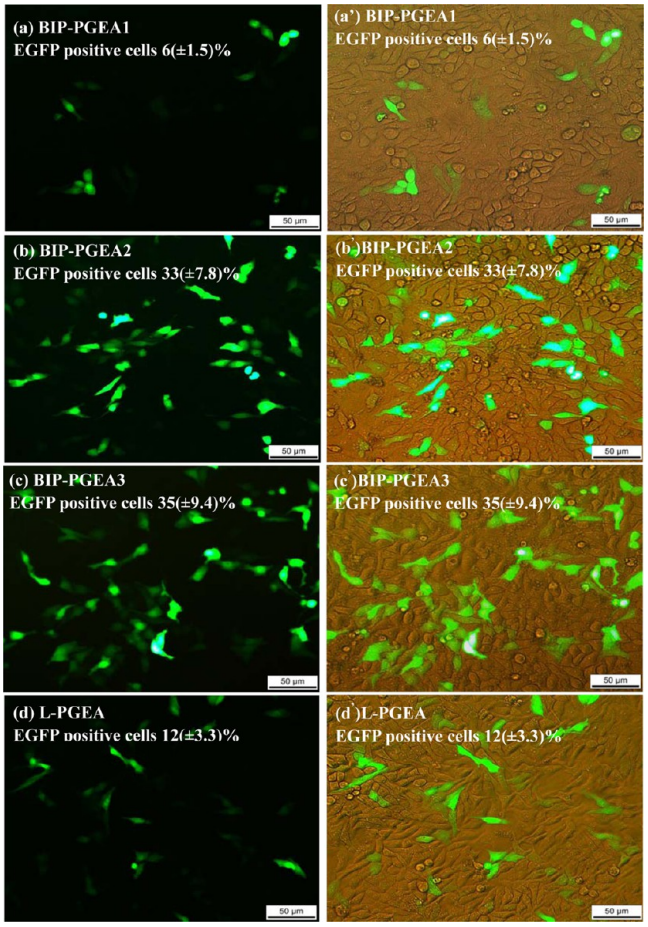

Figure 7. Representative images of EGFP expression mediated by (a, a′) BIP-PGEA1, (b, b′) BIP-PGEA2, (c, c′) BIP-PGEA3 and (d, d′) L-PGEA at the optimal N/P ratio of 25 in HepG2 cells.

determined using flow cytometry, reflected the transfection efficiency. The percentages of the EGFP-positive cells for BIP-PGEA1, BIP-PGEA2, BIP-PGEA3, and L-PGEA were 6 ± 1.5%, 33 ± 1.8%, 35 ± 2.4%, and 12 ± 1.3%, respectively. This result was fairly consistent with those of luciferase expression (Figure 6).

Drug Loading, Release, and Killing Ability. The BIP-PGEA NPs possessed π-conjugated hydrophobic BIP cores. The conjugated structure could attach and absorb aromatic, water insoluble drugs such as 10-hydroxycamptothecin (CPT) via noncovalent van der Waals interactions.[48] Due to its good gene transfection efficiency and low cytotoxicity, BIP-PGEA2 was selected for CPT loading. The UV−vis spectra of BIP-PGEA2 aqueous solutions with or without CPT are shown in Figure 8a. The UV−vis spectra of BIP-PGEA2-CPT at different concentrations clearly revealed the typical absorption peak of CPT (at 380 nm), indicating that CPT was successfully loaded into the BIP-PGEA2 NPs. Based on the extinction coefficients and optical absorbance data of CPT and BIP-PGEA2, it was estimated that 1 g of the BIP-PGEA2 NPs bound approximately 0.1 g of CPT. The good CPT loading ability is likely attributed to the hydrophobic nature of the π-conjugated plane of BIP. The morphology of the BIP-PGEA2-CPT was observed using TEM. BIP-PGEA2-CPT existed in the form of spherical aggregates with diameters of approximately 140 nm in the dry state (Figure 4c). An image of the resultant BIP-PGEA2-CPT/pDNA after complexing with pDNA is shown in Figure 4d.

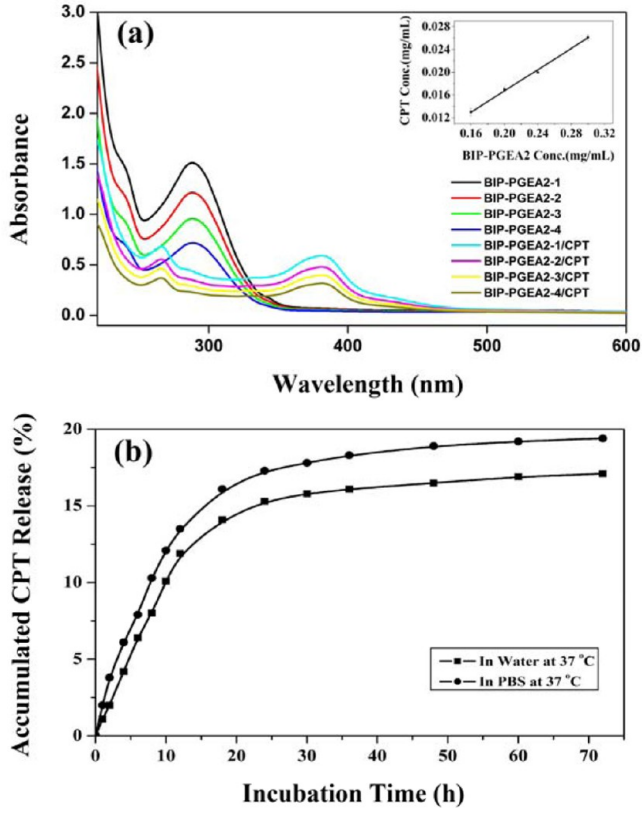

Figure 8. (a) UV−vis absorption spectra of BIP-PGEA2 and BIP-PGEA2-CPT with different concentrations. The inset demonstrates the linear relationship between the drug and carrier concentrations. (b) In vitro release profile of CPT from BIP-PGEA2-CPT. The samples were incubated in water or PBS buffer (pH = 7.4) at 37 °C.

The in vitro release of CPT from BIP-PGEA2-CPT was investigated in PBS (pH 7.4, 37 °C) or water. As shown in Figure 8b, the CPT showed similar release profiles, and the release was sustained over 72 h. The amount of CPT that was released in water and PBS was 17.1 ± 0.51% and 19.4 ± 0.62%, respectively. The low amount of drug release was likely due to the hydrophobic interactions and $\pi-\pi$ stacking between CPT and BIP.

CPT has been widely used for treating many cancers.[49−51] To evaluate the antitumor effectiveness of BIP-PGEA2-CPT, the in vitro cytotoxicity of free CPT and BIP-PGEA2-CPT at different concentrations was assayed using HepG2 cells. The relative cell viability was measured using the standard MTT assay after 72 h of incubation. As shown in Figure 9a, free CPT showed no obvious cytotoxicity. BIP-PGEA2-CPT exhibited a stronger in vitro killing capability for HepG2 cells. In addition, the killing capability of BIP-PGEA2-CPT was dependent on the incubation time. A shorter incubation time led a decreased killing effect, likely due to the decreased amount of CPT released.

In Vitro Antitumor Effect with a 5-FC/ECD Suicide System. A suicide gene/prodrug system has been promising in treating radioresistant and chemoresistant tumors.[32,33] The synergistic antitumor effect of BIP-PGEA-CPT was assayed using a cytosine deaminase/5-fluorocytosine (CD/5-FC) suicide gene system. The CD/5-FC system is one of the most widely and extensively investigated suicide gene/prodrug

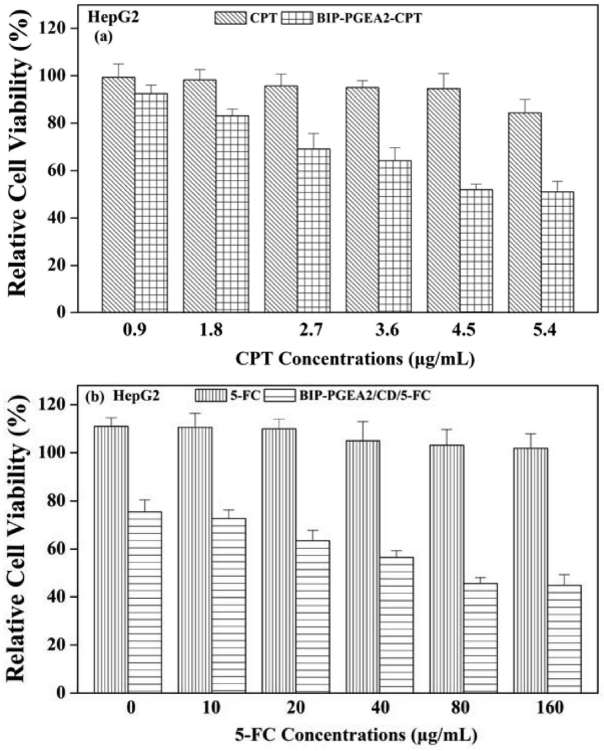

Figure 9. Relative cell viabilities of HepG2 cells treated with different concentrations of (a) free CPT and BIP-PGEA2-CPT and of (b) 5-FC after transfection mediated by BIP-PGEA2/pCMV-CD complexes at a N/P ratio of 25.

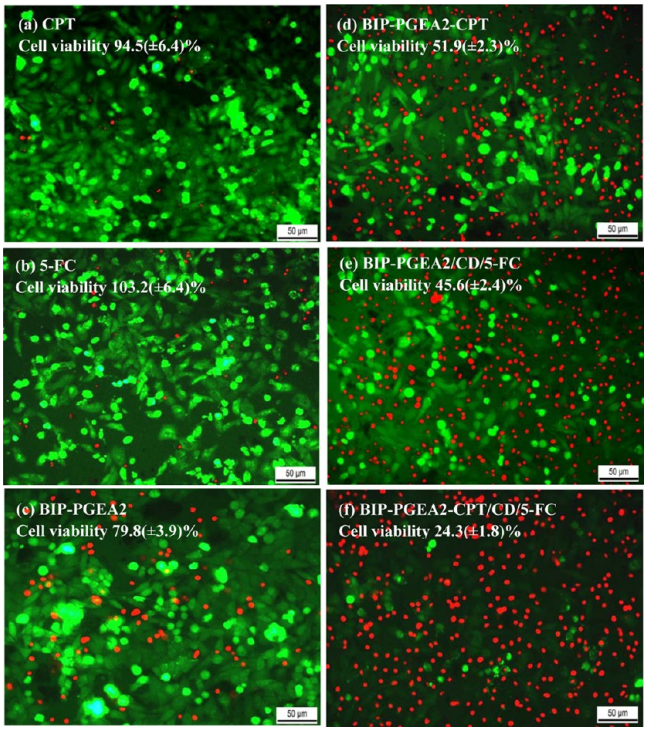

Figure 10. FDA-PI stained HepG2 cells treated with (a) free 5-FC (80 μg/mL), (b) free CPT (4.5 μg/mL, equal to that of CPT in BIP-PGEA2/CPT at a N/P ratio of 25), (c) BIP-PGEA2, (d) BIP-PGEA2-CPT, (e) BIP-PGEA2/CD/5-FC (at a N/P ratio of 25 and a 5-FC concentration of 80 μg/mL), and (f) BIP-PGEA2-CPT/CD/5-FC (at a N/P ratio of 25 and a 5-FC concentration of 80 μg/mL).

systems during the past decade.[52] CD can convert the nontoxic prodrug 5-FC to form the highly cytotoxic 5-fluorouracil (5-FU).

The antitumor effect of BIP-PGEA2/pCMV-CD at its optimal transfection N/P ratio of 25 was first evaluated at various 5-FC concentrations. As shown in Figure 9b, the viability of the HepG2 cells was approximately 100% when treated with 5-FC alone (Figure 10a), indicating that the cytotoxicity of the pro-drug 5-FC was neglectable in HepG2 cells. The HepG2 groups treated with BIP-PGEA2/pCMV-CD showed a substantial decrease in cell viability with increasing 5-FC concentration. Sufficient 5-FC was required for the 5-FC/ECD system to be effective for killing tumor cells. At a 5-FC concentration of 80 μg/mL or higher, the viability of cells treated with BIP-PGEA2/pCMV-CD was less than 45.6%.

To directly observe the in vitro antitumor effect of the 5-FC/ECD system mediated by BIP-PGEA2, FDA-PI staining was used to visualize the cell viability. Figure 10 shows the representative images of HepG2 cells treated with different complexes. Few dead cells were observed in the groups treated with free CPT (Figure 10a) and 5-FC (Figure 10b). Compared with BIP-PGEA2 (Figure 10c), a greater amount of dead cells were observed in the group treated with BIP-PGEA2-CPT (Figure 10d, cell viability: 51.9%). These results were consistent with the corresponding MTT assay (Figure 9). In the presence of 5-FC, in comparison with the group treated with BIP-PGEA2/pCMV-CD (Figure 10e; cell viability, 46%), a significantly higher number of dead cells were observed for BIP-PGEA2-CTP/pCMV-CD (Figure 10f, cell viability: 24%) due to the synergistic antitumor effects of the 5-FC/ECD system and the chemotherapy of the CPT released from BIP-PGEA2-CPT. These results further confirmed the effective antitumor ability of the 5-FC/ECD system mediated by BIP-PGEA2-CTP.

CONCLUSIONS

A series of low molecular weight BIP-PGEAs were successfully prepared via ATRP. BIP-PGEA could form a new type of well-defined cationic nanoparticle for the codelivery of a gene and a drug. The π-conjugated hydrophobic BIP core could entrap an anticancer drug, CPT, whereas the PGEA periphery could efficiently condense pDNA. BIP-PGEA exhibited a significantly higher transfection efficiency than L-PGEA and the traditional "gold-standard" PEI (25 kDa). BIP-PGEA-CPT exhibited an effective synergistic antitumor ability using the 5-FC/ECD suicide gene therapy system. The present work would offer a new strategy for designing multifunctional therapeutic delivery systems with low toxicity and high efficiency.

ASSOCIATED CONTENT

Supporting Information

Typical ^{1}H NMR spectra of BIP-OH, BIP-Br, BIP-PGMA2, and BIP-PGEA2 and the complex stability in serum. This material is available free of charge via the Internet at http://pubs.acs.org.

AUTHOR INFORMATION

Corresponding Authors

*Email: xufj@mail.buct.edu.cn.
*Email: yubr@mail.buct.edu.cn.

Notes

The authors declare no competing financial interest.

■ ACKNOWLEDGMENTS

This work was supported by the National Natural Science Foundation of China (grant Nos. 51173014, 51221002, and 51325304), and the Research Fund for the Doctoral Program of Higher Education of China (project No. 20120010120007).

■ REFERENCES

(1) Verma, I. M.; Somia, N. Gene Therapy—Promises, Problems, and Prospects. *Nature* **1997**, *389*, 239−242.
(2) Edelstein, M. L.; Abedi, M. R.; Wixon, J. Gene Therapy Clinical Trials Worldwide to 2007: An Update. *J. Gene Med.* **2007**, *9*, 833−842.
(3) Meng, F. H.; Hennink, W. E.; Zhong, Z. Y. Reduction-Sensitive Polymers and Bioconjugates for Biomedical Applications. *Biomaterials* **2009**, *30*, 2180−2198.
(4) Tang, L. Y.; Wang, Y. C.; Li, Y.; Du, J. Z.; Wang, J. Micelles Based on Disulfide-Linked Block Copolymer as Potential Carrier for Intracellular Drug Delivery. *Bioconjugate Chem.* **2009**, *20*, 1095−1099.
(5) He, Y. Y.; Nie, Y.; Cheng, G.; Xie, L.; Shen, Y. Q.; Gu, Z. W. Viral Mimicking Ternary Polyplexes: A Reduction-Controlled Hierarchical Unpacking Vector for Gene Delivery. *Adv. Mater.* **2013**, *26*, 1534−1540.
(6) Duan, X.; Wang, M.; Men, P. K.; Gao, X.; Huang, M. J.; Gou, M. L.; Chen, L. J.; Qian, Z. Y.; Wei, Y. Q. Treating Colon Cancer With a Suicide Gene Delivered by Self-Assembled Cationic MPEG-PCL Micelles. *Nanoscale* **2012**, *4*, 2400−2047.
(7) Busseron, E.; Ruff, Y.; Moulin, E.; Giuseppone, N. Supramolecular Self-Assemblies as Functional Nanomaterials. *Nanoscale* **2013**, *5*, 7098−7140.
(8) Mintzer, M. A.; Simanek, E. E. Nonviral Vectors for Gene Delivery. *Chem. Rev.* **2009**, *109*, 259−302.
(9) Xu, F. J.; Yang, W. T. Polymer Vectors via Controlled/Living Radical Polymerization for Gene Delivery. *Prog. Polym. Sci.* **2011**, *36*, 1099−1131.
(10) Pathak, A.; Kumar, P.; Chuttani, K.; Jain, S.; Mishra, A. K.; Vyas, S. P.; Gupta, K. C. Gene Expression, Biodistribution, and Pharmacoscintigraphic Evaluation of Chondroitin Sulfate-PEI Nanoconstructs Mediated Tumor Gene Therapy. *ACS Nano* **2009**, *3*, 1493−1505.
(11) Kim, H.; Kim, W. J. Photothermally Controlled Gene Delivery by Reduced Graphene Oxide−Polyethylenimine Nanocomposite. *Small* **2014**, *10*, 117−126.
(12) Tian, H. Y.; Lin, L.; Chen, J.; Chen, X. S.; Park, T. G.; Maruyama, A. RGD Targeting Hyaluronic Acid Coating System for PEI-PBLG Polycation Gene Carriers. *J. Controlled Release* **2011**, *155*, 47−53.
(13) Wang, H. Y.; Yi, W. J.; Qin, S. Y.; Li, C.; Zhuo, R. X.; Zhang, X. Z. Tyroserleutide-Based Gene Vector for Suppressing VEGF Expression in Cancer Therapy. *Biomaterials* **2012**, *33*, 8685−8694.
(14) Li, J. G.; Cheng, D.; Yin, T. H.; Chen, W. C.; Lin, Y. J.; Chen, J. F.; Li, R. T.; Shuai, X. T. Copolymer of Poly(ethylene glycol) and Poly(L-lysine) Grafting Polyethylenimine through a Reducible Disulfide Linkage for siRNA Delivery. *Nanoscale* **2014**, *6*, 1732−1740.
(15) Dai, F. Y.; Sun, P.; Liu, Y. J.; Liu, W. G. Redox-Cleavable Star Cationic PDMAEMA by Arm-First Approach of ATRP as a Nonviral Vector for Gene Delivery. *Biomaterials* **2010**, *31*, 559−569.
(16) Yan, Y. S.; Wei, D. X.; Li, J. Y.; Zheng, J. H.; Shi, G. G.; Luo, W. H.; Pan, Y.; Wang, J. Z.; Zhang, L. M.; He, X. Y.; Liu, D. J. A Poly(L-lysine)-Based Hydrophilic Star Block Co-Polymer as a Protein Nanocarrier with Facile Encapsulation and pH-Responsive Release. *Acta Biomater.* **2012**, *8*, 2113−2120.
(17) Uchida, H.; Miyata, K.; Oba, M.; Ishii, T.; Suma, T.; Itaka, K.; Nishiyama, N.; Kataoka, K. Odd-Even Effect of Repeating Aminoethylene Units in the Side Chain of N-Substituted Polyaspartamides on Gene Transfection Profiles. *J. Am. Chem. Soc.* **2011**, *133*, 15524−15532.
(18) Zhu, Y.; Tang, G. P.; Xu, F. J. Efficient Poly(N-3-hydroxypropyl) as Partamide-Based Carriers via ATRP for Gene Delivery. *ACS Appl. Mater. Interfaces* **2013**, *5*, 1840−1848.
(19) Kukowska-Latallo, J. F.; Bielinska, A. U.; Johnson, J.; Spindler, R.; Tomalia, D. A.; Baker, J. R. Efficient Transfer of Genetic Material into Mammalian Cells Using Starburst Polyamidoamine Dendrimers. *Proc. Natl. Acad. Sci. U.S.A.* **1996**, *93*, 4897−4902.
(20) Chai, M. Y.; Li, W. B.; Ping, Y.; Tang, G. P.; Yang, W. T.; Ma, J.; Liu, F. S. Well-Defined Poly(2-hydroxyl-3-(2-hydroxyethlamino)-propyl methacylate) Vectors with Low Cytotoxicity and High Gene Transfection Efficiency. *Biomacromolecules* **2010**, *11*, 1437−1442.
(21) Hu, Y.; Zhu, Y.; Yang, W. T.; Xu, F. J. New Star-Shaped Carriers Composed of β-Cyclodextrin Cores and Disulfi de-Linked Poly-(glycidyl methacrylate) Derivative Arms with Plentiful Flanking Secondary Amine and Hydroxyl Groups for Highly Efficient Gene Delivery. *ACS Appl. Mater. Interfaces* **2013**, *5*, 703−712.
(22) Liang, Z. X.; Wu, X. S.; Yang, Y. W.; Li, C.; Wu, G. L.; Gao, H. Quaternized Amino Poly(glycerol-methacrylate)s for Enhanced pDNA Delivery. *Polym. Chem.* **2013**, *4*, 3514−3523.
(23) Li, C.; Yang, Y. W.; Liang, Z. X.; Wu, G. L.; Gao, H. Post-Modification of Poly(glycidyl methacrylate)s with Alkyl Amine and Isothiocyanate for Effective pDNA Delivery. *Polym. Chem.* **2013**, *4*, 4366−4374.
(24) Li, Q. L.; Gu, W. X.; Gao, H.; Yang, Y. W. Self-Assembly and Applications of Poly(glycidyl methacrylate)s and Their Derivatives. *Chem. Commun.* **2014**, DOI: 10.1039/c4cc03036b.
(25) Li, Q. L.; Wang, L. Z.; Qiu, X. L.; Sun, Y. L.; Wang, P. X.; Liu, Y.; Li, F.; Qi, A. D.; Gao, H.; Yang, Y. W. Stimuli-Responsive Biocompatible Nanovalvesbased on β-Cyclodextrin Modified Poly-(glycidylmethacrylate). *Polym. Chem.* **2014**, *5*, 3389−3395.
(26) Nguyen, J.; Szoka, F. C. Nucleic Acid Delivery: The Missing Pieces of the Puzzle. *Acc. Chem. Res.* **2012**, *45*, 1153−1162.
(27) Won, Y. Y.; Sharma, R.; Konieczny, S. F. Missing Pieces in Understanding the Intracellular Trafficking of Polycation/DNA Complexes. *J. Controlled Release* **2009**, *139*, 88−93.
(28) Morin, E.; Nothisen, M.; Wagner, A.; Remy, J. S. Cationic Polydiacetylene Micelles for Gene Delivery. *Bioconjugate Chem.* **2011**, *22*, 1916−1923.
(29) Yang, X. C.; Zhao, N. N.; Xu, F. J. Biocleavable Graphene Oxide Based-Nanohybrids Synthesized via ATRP for Gene/Drug Delivery. *Nanoscale* **2014**, *6*, 6141−6150.
(30) Hu, H.; Xiu, K. M.; Xu, S. L.; Yang, W. T.; Xu, F. J. Functionalized Layered Double Hydroxide Nanoparticles Conjugated with Disulfide-Linked Polycation Brushes for Advanced Gene Delivery. *Bioconjugate Chem.* **2013**, *24*, 968−978.
(31) Lu, X.; Ping, Y.; Xu, F. J.; Li, Z. H.; Wang, Q. Q.; Chen, J. H.; Yang, W. T.; Tang, G. P. Bifunctional Conjugates Comprising β-Cyclodextrin, Polyethylenimine, and 5-Fluoro-2′- Deoxyuridine for Drug Delivery and Gene Transfer. *Bioconjugate Chem.* **2010**, *21*, 1855−1863.
(32) Lu, X.; Wang, Q. Q.; Xu, F. J.; Tang, G. P.; Yang, W. T. A Cationic Prodrug/Therapeutic Gene Nanocomplex for the Synergistic Treatment of Tumors. *Biomaterials* **2011**, *32*, 4849−4856.
(33) Xu, Q. X.; Leong, J. Y.; Chua, Q. Y.; Chi, Y. T.; Chow, P. K. H.; Pack, D. W.; Wang, C. H. Combined Modality Doxorubicin-Based Chemotherapy and Chitosan-Mediated p53 Gene Therapy Using Double-Walled Microspheres for Treatment of Human Hepatocellular Carcinoma. *Biomaterials* **2013**, *34*, 5149−5162.
(34) Wiradharma, N.; Tong, Y. W.; Yang, Y. Y. Self-Assembled Oligopeptide Nanostructures for Co-Delivery of Drug and Gene with Synergistic Therapeutic Effect. *Biomaterials* **2009**, *30*, 3100−3109.
(35) Zhao, F.; Yin, H.; Li, J. Supramolecular Self-Assembly Forming a Multifunctional Synergistic System for Targeted Co-Delivery of Gene and Drug. *Biomaterials* **2014**, *35*, 1050−1062.
(36) Ichikawa, T.; Tamiya, T.; Adachi, Y.; Ono, Y.; Matsumoto, K.; Furuta, T.; Yoshida, Y.; Hamada, H.; Ohmoto, T. In Vivo Efficacy and Toxicity of 5-Fluorocytosine/Cytosine Deaminase Gene Therapy for Malignant Gliomas Mediated by Adenovirus. *Cancer Gene Ther.* **2000**, *7*, 74−82.
(37) Lawrence, T. S.; Rehemtulla, A.; Ng, E. Y.; Wilson, M.; Trosko, J. E.; Stetson, P. L. Preferential Cytotoxicity of Cells Transduced With

Cytosine Deaminase Compared to Bystander Cells after Treatment with 5-Flucytosine. *Cancer Res.* **1998**, *58*, 2588−2593.
(38) Welterlich, I.; Tieke, B. Conjugated Polymer with Benzimidazolyl Pyridine Ligands in the Side Chain: Metal Ion Coordination and Coordinative Self-assembly into Fluorescent Ultrathin Films. *Macromolecules* **2011**, *44*, 4194−4203.
(39) Xu, F. J.; Li, H. Z.; Li, J.; Zhang, Z. X.; Kang, E. T.; Neoh, K. G. Pentablock Copolymers of Poly(ethylene glycol), Poly((2-dimethyl amino)ethyl methacrylate) and Poly(2-hydroxyethyl methacrylate) from Consecutive Atom Transfer Radical Polymerizations for Non-Viral Gene Delivery. *Biomaterials* **2008**, *29*, 3023−3033.
(40) Yang, Y. Y.; Wang, X.; Hu, Y.; Hu, H.; Wu, D. C.; Xu, F. J. Bioreducible POSS-Cored Star-Shaped Polycation for Efficient Gene Delivery. *ACS Appl. Mater. Interfaces* **2014**, *6*, 1044−1052.
(41) Pan, Y. Z.; Bao, H. Q.; Sahoo, N. G.; Wu, T. F.; Li, L. Water-Soluble Poly(N-isopropylacrylamide)−Graphene Sheets Synthesized via Click Chemistry for Drug Delivery. *Adv. Funct. Mater.* **2011**, *21*, 2754−2763.
(42) Feng, X. L.; Lv, F. T.; Liu, L. B.; Tang, H. W.; Xing, C. F.; Yang, Q.; Wang, S. Conjugated Polymer Nanoparticles for Drug Delivery and Imaging. *ACS Appl. Mater. Interfaces* **2010**, *2*, 2429−2435.
(43) Lale, S. V.; Aswathy, R. G.; Aravind, A.; Kumar, D. S.; Koul, V. AS1411 Aptamer and Folic Acid Functionalized pH-Responsive ATRP Fabricated pPEGM −PCL−pPEGMA Polymeric Nanoparticles for Targeted Drug Delivery in Cancer Therapy. *Biomacromolecules* **2014**, *15*, 1737−1752.
(44) Dou, X. B.; Hu, Y.; Zhao, N. N.; Xu, F. J. Different Types of Degradable Vectors from Low-Molecular-Weight Polycation-Functionalized Poly(aspartic acid) for Efficient Gene Delivery. *Biomaterials* **2014**, *35*, 3015−3026.
(45) Hu, Y.; Chai, M. Y.; Yang, W. T.; Xu, F. J. Supramolecular Host−Guest Pseudocomb Conjugates Composed of Multiple Star Polycations Tied Tunably with a Linear Polycation Backbone for Gene Transfection. *Bioconjugate Chem.* **2013**, *24*, 1049−1056.
(46) Wetering, P. V. D.; Moret, E. E.; Nieuwenbroek, N. M. E.; Steenbergen, M. J. V.; Hennink, W. E. Structure−Activity Relationships of Water-Soluble Cationic Methacrylate/Methacrylamide Polymers for Nonviral Gene Delivery. *Bioconjugate Chem.* **1999**, *10*, 589−597.
(47) Li, R. Q.; Hu, Y.; Yu, B. R.; Zhao, N. N.; Xu, F. J. Bioreducible Comb-Shaped Conjugates Composed of Secondary Amine and Hydroxyl Group-Containing Backbones and Disulfide-Linked Side Chains with Tertiary Amine Groups for Facilitating GeneDelivery. *Bioconjugate Chem.* **2014**, *25*, 155−164.
(48) Pan, Y. Z.; Bao, H. Q.; Sahoo, N. G.; Wu, T. F.; Li, L. Water-Soluble Poly(N-isopropylacrylamide)−Graphene Sheets Synthesized via Click Chemistry for Drug Delivery. *Adv. Funct. Mater.* **2011**, *21*, 2754−2763.
(49) Hsiang, Y. H.; Liu, L. F.; Wall, M. E.; Wani, M. C.; Nicholas, A. W.; Manikumar, G.; Kirschenbaum; Silber, S. R.; Potmesil, M. DNA Topoisomerase I-Mediated DNA Cleavage and Cytotoxicity of Camptothecin Analogues. *Cancer Res.* **1989**, *49*, 4385−4389.
(50) Lee, M. H.; Kim, J. Y.; Han, J. H.; Bhuniya, S.; Sessler, J. L.; Kang, C.; Kim, J. S. Direct Fluorescence Monitoring of the Delivery and Cellular Uptake of a Cancer-Targeted RGD Peptide-Appended Naphthalimide Theragnostic Prodrug. *J. Am. Chem. Soc.* **2012**, *134*, 12668−12674.
(51) Wang, J. Q.; Sun, X. R.; Mao, W. W.; Sun, W. L.; Tang, J. B.; Sui, M. H.; Shen, Y. Q.; Gu, Z. W. Tumor Redox Heterogeneity-Responsive Prodrug Nanocapsules for Cancer Chemotherapy. *Adv. Mater.* **2013**, *25*, 3670−3676.
(52) Liang, B.; He, M. L.; Chan, C. Y.; Chen, Y. C.; Li, X. P.; Li, Y.; Zheng, D. X.; Lin, M. C.; Kung, H. F.; Shuaib, X. T.; Peng, Y. The Use of Folate-PEG-Grafted- Hybranched-PEI Non-Viral Vector for the Inhibition of Glioma Growth in the Rat. *Biomaterials* **2009**, *30*, 4014−4020.